Crystal Structures of Encapsulates within Zeolites. 3. Xenon in Zeolite A

Nam Ho Heo,* Woo Taik Lim, Bok Jo Kim, Sang Yeon Lee, Myung Chul Kim,† and Karl Seff*,‡

Department of Industrial Chemistry, Kyungpook National University, Taegu 702-701, Korea

Received: May 19, 1998; In Final Form: December 31, 1998

The positions of Xe atoms encapsulated in the cavities of fully dehydrated zeolite A of unit-cell composition $Cs_3Na_8HSi_{12}Al_{12}O_{48}$ (Cs_3-A) have been determined. Cs_3-A was exposed to 255 atm of xenon at 400 °C for 7 days, followed by cooling at pressure to encapsulate Xe atoms; a second crystal was treated similarly at 450 atm, and a third at 1020 atm. The resulting crystal structures of Cs_3-A(2.5Xe) (crystal 1, $a = 12.245(2)$ Å, $R_1 = 0.056$, $R_2 = 0.059$), Cs_3-A(4.5Xe) (crystal 2, $a = 12.258(2)$ Å, $R_1 = 0.061$, $R_2 = 0.058$), and Cs_3-A(5.25Xe) (crystal 3, $a = 12.236(2)$ Å, $R_1 = 0.061$, $R_2 = 0.057$) were determined by single-crystal X-ray diffraction techniques in the cubic space group *Pm*3*m* at 21(1) °C and 1 atm. The approximately 2.5, 4.5, and 5.25 Xe atoms per unit cell, respectively, are distributed over three crystallographically distinct positions. At the center of each sodalite unit in crystals 1, 2, and 3, respectively, are 0.5, 0.75, and 0.75 Xe atoms at Xe(1); in addition, off center in crystal 3 are 0.25 Xe atoms at Xe(4), opposite a six-ring in the sodalite unit. Opposite four-rings in the large cavity at Xe(2) are 1, 2, and 2.25 Xe atoms, respectively, for the three crystals. Opposite six-rings in the large cavity at Xe(3) are 1, 1.75, and 2 Xe atoms, respectively. Relatively strong interactions of Xe(3) atoms with six-ring Na^+ ions are observed: Na−Xe(3) = 3.18(2), 3.22(2), and 3.38(2) Å, respectively. In Cs_3-A(2.5Xe), two Xe atoms are found in each large cavity: Xe_2 with a 4.54(4) Å distance may exist. Cs_3-A(4.5Xe) may be viewed as a mixture of two kinds of unit cells: in most of their large cavities, four Xe atoms form a rhombus with Xe(2)−Xe(3) = 4.51(3) Å and Xe(2)−Xe(3)−Xe(2) = 95.1(5)°. Cs_3-A(5.25Xe) may also be viewed as having two kinds of large cavities: 75% contain a rhombus of four Xe atoms, Xe(2)−Xe(3) = 4.45(2) Å and Xe(2)−Xe(3)−Xe(2) = 97.3(4)°. The remaining 25% have five Xe atoms arranged trigonal-bipyramidally with three Xe(2)'s equatorial and two Xe(3)'s axial (Xe(2)−Xe(3) = 4.45(2) Å). These arrangements of encapsulated Xe atoms in the large cavity are stabilized by alternating dipoles induced on Xe(2) and Xe(3) atoms by four-ring oxygens and six-ring Na^+ ions, respectively.

Introduction

Since Fraissard's pioneering work,[1] ^{129}Xe NMR spectroscopy has been widely used as a probe for studying the pore structure of zeolites and other porous materials. Xenon's chemical inertness and high polarizability allow it to be particularly sensitive to its environment. The positions and widths of the ^{129}Xe NMR lines depend on the collisions of xenon atoms with each other, with the walls of the zeolite, and with atoms of supported materials: this allows structural information to be obtained. For nonzeolitic porous materials, the short-range crystallinity[2] and the chemical nature of various supported materials before and after chemisorption of a gas can be determined.[1] For zeolites, various physicochemical information regarding the electrical and magnetic effects of cations[2] and their migration processes,[3−5] and the nature of guest species such as metal clusters,[6] sorbed phases,[7,8] and coke deposits,[9] can be learned.

Li and Berry[10] used NOSE isothermal molecular dynamics simulations[11] to study the dynamics of various numbers of Xe atoms inside a single α-cage of Na-A at various temperatures. They divided the cavity into several sites according to the potentials of interaction of these sites with a single Xe atom inside the cavity and analyzed the dynamics of occupation of these sites by Xe atoms. They attempted to explain the NMR spectra of ^{129}Xe atoms in Na-A as a function of cluster size and temperature.

Jameson et al.[11−13] studied the equilibrium distribution of the Xe atoms among the α-cages of Na-A at xenon loadings ranging from very low to saturation by ^{129}Xe NMR. They observed Xe atoms trapped in the α-cages of Na-A in their ^{129}Xe spectrum. They then compared these results with simulations done using a Grand Canonical Monte Carlo (GCMC) method. Their GCMC, hypergeometric distribution, and continuum models were in quantitative agreement with the distribution of Xe atoms observed experimentally by NMR. They actually found 11 local minima for a single Xe atom and some minimum energy configurations for Xe_2 to Xe_8 in the α-cage. No Xe atom was found under any circumstances in the middle of the α-cage.[12,13] They also calculated the minimum energy sorption sites, the one-body distribution functions, and the pair distribution functions: these provide a physical picture of the structure of the sorbed xenon.

The utilization of zeolites as a storage medium for neon,[14] argon,[14,15] krypton,[14] dinitrogen,[15] carbon dioxide,[15] methane,[16,17] dihydrogen,[18−20] and xenon[21] was extensively examined using various cations to block the windows of the zeolite. In particular, Samant et al.[21] studied xenon atoms sorbed in the α-cages of Na-A at 525 K and 40 bar, resulting in up to 1.8 atoms per

† College of General Education, Kyung-il University, Kyungsan 712-701, Korea.

‡ Department of Chemistry, University of Hawaii at Manoa, Honolulu, Hawaii 96822-2275.

10.1021/jp982300x CCC: $18.00 © 1999 American Chemical Society
Published on Web 03/02/1999

cage, by ^{129}Xe NMR. Their work showed that the ^{129}Xe chemical shift in a cavity smaller than the mean free path of xenon in the gas phase at the pressure of the experiment is a function of the size of the cavity and suggested that the peaks appearing at higher chemical shift correspond to an increasing number of xenon atoms per α-cage. By studying the ^{129}Xe NMR spectrum of the sample saturated with water by exposure to excess water at room temperature, they showed that a xenon−water clathrate had formed, and suggested that the desorption of xenon from the zeolite upon water addition is probably due to solvation of the zeolitic cations, resulting in an opening of the apertures to the α-cages.

Dooryhee et al.[22] had suggested, following synchrotron X-ray diffraction studies of Xe with Na-X at 31 °C at 1.0 and 1.75 atm, that the predominant site for Xe is in association with Na^+ ions in six-membered rings of the α-cage. However, a molecular dynamics study by Santikary et al.[23] had concluded that the primary adsorption site is near the middle of a four-membered ring at the low loading of one Xe atom per α-cage.

Derouane and B'Nagy[24,25] related δ_s, which is characterized as the specific physical interaction between sorbed xenon and the wall of the void space, with the surface curvature in calculating the physisorption energy. The sorbed xenon was required to remain near the surface in their model. Although the cage wall is theoretically the energetically most favorable position for sorption, direct experimental evidence for this was lacking.

In recent years, the Kr_4, Ar_4, and Ar_5 clusters, formed by confinement in the cavities of Cs_3Na_8H-A (Cs_3-A),[26,27] were characterized crystallographically.[28,29] In the structures of Cs_3-A(5Kr) and Cs_3-A(5Ar), four Kr or Ar atoms in each large cavity form a rhombus with interatomic distances of 4.67(3) and 4.75(8) Å, respectively, and angles of 95.6(5)° and 87.6(14)° for Kr(2)−Kr(3)−Kr(2) and Ar(2)−Ar(3)−Ar(2), respectively. The five Ar atoms in the large cavity of Cs_3-A(6Ar) have a trigonal-bipyramidal arrangement with three Ar(2) atoms at equatorial positions and two Ar(3) atoms at axial positions: Ar(2)−Ar(3) = 4.63(9), Ar(2)−Ar(2) = 5.80(9) Å, and Ar(2)−Ar(3)−Ar(2) = 78(2)°. In these clusters, charge dipoles induced on the rare gas atoms by their interactions with the zeolite alternate around the ring, showing the effect of the electrostatic fields in the zeolite cavity.

Without direct evidence, most scientists working on xenon occlusion into zeolites by ^{129}Xe NMR, Grand Canonical Monte Carlo Simulation (GCMC), and Molecular Dynamics Simulation have assumed that Xe atoms (kinetic diameter = 3.96 Å)[30] could not gain access to the sodalite cavities whose windows have a free diameter of only ca. 2.2 Å.[1,12,21,31] However, in the crystal structures of Cs_3-A(*x*Ar), $x = 5$ or 6,[29] and Cs_3-A(5Kr),[28] one Ar (kinetic diameter = 3.40 Å)[30] or Kr atom (3.60 Å)[30] was always and unambiguously found near the center of each sodalite unit, indicating that one or more dynamic processes exist for the passage of those atoms through six-rings, at least at elevated temperatures, even though their aperture is formally considered to be too small.

In this work, xenon atoms were encapsulated at various pressures in the cavities of fully dehydrated Cs_3-A[26−29] in order to observe their positions and to further characterize the confinement effect[28,29] crystallographically. Both the Cs^+ and Na^+ ions of Cs_3-A were expected to contribute to the effective encapsulation of Xe atoms by blocking the eight- and six-rings, respectively.[19,27−29,32−36] Although weak interactions were expected, the precise coordinates of the encapsulated Xe atoms, sensitive to the electrostatic field in a relatively unperturbed zeolite, would be seen. Perhaps interesting clusters of Xe atoms in the large cavity, and a Xe atom despite its size in the sodalite unit, would be seen.

Experimental Section

Colorless single crystals of zeolite 4A, $Na_{12}Si_{12}Al_{12}O_{48}\cdot 27H_2O$ (Na_{12}-A·$27H_2O$),[26] were synthesized by Kokotailo and Charnell.[37] Crystals of hydrated Cs_3-A (approximate composition Cs_3Na_8H-A) were prepared by dynamic (flow) ion exchange with an aqueous solution (pH = 5.7), 0.04 M in Cs^+ and 0.06 M in Na^+ made by using $CsNO_3$ and $NaNO_3$ (both Aldrich 99.99%). This solution composition was carefully chosen so that all eight- and six-ring sites of the zeolite would be fully occupied by Cs^+ and Na^+ ions with occupancies of 3.0 and 8.0 per unit cell, respectively.[27−29] A single crystal of hydrated Cs_3-A (crystal 1), a cube 80 μm on an edge, was lodged in a fine Pyrex capillary with both ends open. This capillary was transferred to a high-pressure line connected to the vacuum line. After cautious increases in temperature of 25 °C/h under vacuum, followed by complete dehydration at 400 °C and 1×10^{-4} Torr for 2 days, Xe sorption into the crystal was done at 400 °C for 7 days with 255 atm of Xe (Matheson, 99.996%). This pressure of xenon gas was produced by condensing the gas in the high-pressure chamber (immersed in a liquid-nitrogen bath) which contained the Cs_3-A crystal in its capillary, followed by reheating to appropriate temperature after isolating the chamber from the vacuum line. Encapsulation was accomplished by cooling the chamber at pressure to room temperature with an electric fan. The higher loadings of Xe into Cs_3-A (crystals 2 and 3) were achieved similarly with 450 and 1020 atm of Xe, respectively. Following the release of Xe gas from the chamber, both ends of the capillary were presealed with vacuum grease under nitrogen before being completely sealed with a small torch. No changes were noted in the appearance of the crystals upon examination by microscope. The cubic space group *Pm*3*m* (no systematic absences) was used in this work for reasons discussed previously.[38,39] For each crystal, the cell constants, $a = 12.245(2)$, 12.258(2), and 12.236(2) Å, respectively for crystals 1, 2, and 3, at 21(1) °C, were determined by a least-squares treatment of 15 intense reflections for which $20° < 2\theta < 30°$. Each reflection was scanned at a constant scan speed of 0.5°/min in 2θ with a scan width of $(0.46 + 0.63 \tan \theta)$, $(0.91 + 0.92 \tan \theta)$, and $(0.46 + 0.66 \tan \theta)°$, for crystals 1, 2, and 3, respectively. Background intensity was counted at each end of a scan range for a time equal to half the scan time. The intensities of all lattice points for which $2\theta < 70°$ were recorded. Absorption corrections (μR ca. 0.24, 0.28, and 0.29 for crystals 1, 2, and 3,[40] respectively) were judged to be negligible for these crystals, since semiempirical ψ-scans showed only negligible fluctuations for several reflections. Only those reflections in each final data set for which the net count exceeded three times its standard deviation were used in structure solution and refinement. This amounted to 225, 191, and 216 reflections for crystals 1, 2, and 3, respectively. Other crystallographic details are the same as previously reported.[28,29]

Structure Determination

Cs_3-A(2.5Xe) (Crystal 1). Full-matrix least-squares refinement[41] was initiated with the atomic parameters of all framework atoms [(Si,Al), O(1), O(2), and O(3)], Cs^+ at Cs, and Na^+ at Na in Cs_3Na_8H-A.[27−29] A refinement with anisotropic thermal parameters for all atoms converged quickly to the error indices $R_1 = \sum||F_o| - |F_c||/\sum F_o = 0.13$ and $R_2 = (\sum w(F_o - |F_c|)^2/\sum wF_o^2)^{1/2} = 0.18$ with occupancies of 3.09(6) at Cs and 6.8(4)

TABLE 1: Positional, Thermal, and Occupancy Parameters[a]

	Wyckoff position	*x*	*y*	*z*	U_{11} or U_{iso}[b]	U_{22}	U_{33}	U_{12}	U_{13}	U_{23}	occupancy[c] fixed	occupancy[c] varied
(a) Cs_3Na_8H-A(2.5Xe), Crystal 1												
(Si,Al)	24(*k*)	0	1833(3)	3710(2)	14(1)	16(1)	9(1)	0	0	1(1)	24[d]	
O(1)	12(*h*)	0	2224(10)	5000[e]	42(8)	37(7)	17(6)	0	0	0	12	
O(2)	12(*i*)	0	2932(7)	2932(7)	44(8)	22(4)	22(4)	0	0	12(6)	12	
O(3)	24(*m*)	1121(4)	1121(4)	3385(6)	28(3)	28(3)	35(5)	−1(4)	5(3)	5(3)	24	
Cs	3(*c*)	0	5000[e]	5000[e]	108(3)	65(1)	65(1)	0	0	0	3	2.91(3)
Na	8(*g*)	2026(6)	2026(6)	2026(6)	71(3)	71(3)	71(3)	55(3)	55(3)	55(3)	8	8.1(2)
Xe(1)	1(*a*)	0	0	0	639(52)						0.5	0.51(4)
Xe(2)	12(*j*)	3099(18)	3099(18)	5000[e]	112(15)	112(15)	282(42)	−26(22)	0	0	1	1.13(9)
Xe(3)	8(*g*)	3525(23)	3525(23)	3525(23)	386(28)	386(28)	386(28)	−88(27)	−88(27)	−88(27)	1	1.04(9)
(b) Cs_3Na_8H-A(4.5Xe), Crystal 2												
(Si,Al)	24(*k*)	0	1836(3)	3710(3)	14(2)	12(2)	7(2)	0	0	1(2)	24[d]	
O(1)	12(*h*)	0	2234(12)	5000[e]	51(10)	43(9)	11(7)	0	0	0	12	
O(2)	12(*i*)	0	2939(8)	2939(8)	53(10)	23(5)	23(5)	0	0	12(7)	12	
O(3)	24(*m*)	1121(5)	1121(5)	3378(7)	29(4)	29(4)	36(6)	4(5)	4(4)	4(4)	24	
Cs	3(*c*)	0	5000[e]	5000[e]	87(3)	59(2)	59(2)	0	0	0	3	3.11(4)
Na	8(*g*)	2050(7)	2050(7)	2050(7)	71(3)	71(3)	71(3)	62(4)	62(4)	62(4)	8	7.9(3)
Xe(1)	1(*a*)	0	0	0	703(46)						0.75	0.77(3)
Xe(2)	12(*j*)	3080(14)	3080(14)	5000[e]	156(12)	156(12)	348(32)	−70(19)	0	0	2	2.09(5)
Xe(3)	8(*g*)	3567(13)	3567(13)	3567(13)	489(19)	489(19)	489(19)	−185(13)	−185(13)	−185(13)	1.75	1.66(5)
(c) Cs_3Na_8H-A(5.25Xe), Crystal 3												
(Si,Al)	24(*k*)	0	1830(3)	3702(3)	19(1)	16(1)	5(1)	0	0	1(2)	24[d]	
O(1)	12(*h*)	0	2205(10)	5000[e]	38(7)	37(7)	14(6)	0	0	0	12	
O(2)	12(*i*)	0	2939(7)	2939(7)	45(8)	22(4)	22(4)	0	0	12(6)	12	
O(3)	24(*m*)	1119(4)	1119(4)	3370(6)	26(3)	26(3)	33(5)	12(4)	6(3)	6(3)	24	
Cs	3(*c*)	0	5000[e]	5000[e]	101(3)	60(1)	60(1)	0	0	0	3	2.94(7)
Na(1)	8(*g*)	2018(6)	2018(6)	2018(6)	37(3)	37(3)	37(3)	25(3)	25(3)	25(3)	6.5	6.1(2)
Na(2)	8(*g*)	2518(37)	2518(37)	2518(37)	112(12)	112(12)	112(12)	123(14)	123(14)	123(134)	1.5	1.7(1)
Xe(1)	1(*a*)	0	0	0	503(26)						0.75	0.72(2)
Xe(2)	12(*j*)	3071(10)	3071(10)	5000[e]	129(9)	129(9)	731(47)	−35(14)	0	0	2.25	2.26(6)
Xe(3)	8(*g*)	3615(10)	3615(10)	3615(10)	648(14)	648(14)	648(14)	−283(8)	−283(8)	−283(8)	2	2.15(6)
Xe(4)	8(*g*)	816(19)	816(19)	816(19)	116(14)	116(14)	116(14)	−75(8)	−75(8)	−75(8)	0.25	0.22(2)

[a] Positional parameters × 10^4 and thermal parameters × 10^3 are given. Numbers in parentheses are the estimated standard deviations in the units of the least significant figure given for the corresponding parameter. The anisotropic temperature factor is $\exp[-2\pi^2a^{-2}(U_{11}h^2 + U_{22}k^2 + U_{33}l^2 + 2U_{12}hk + 2U_{13}hl + 2U_{23}kl)]$. [b] Isotropic thermal parameters in units of Å^2. Xe(1) is isotropic by symmetry. [c] Occupancy factors are given as the number of atoms or ions per unit cell. [d] Occupancy for (Si) = 12, occupancy for (Al) = 12. [e] Exactly 0.5 by symmetry.

at Na. A difference Fourier function based on this model revealed several peaks deep in the large cavity. A subsequent refinement of a peak on the 3-fold axis opposite a six-ring in large cavity as Xe(3) (see Table 1) converged with the error indices $R_1 = 0.107$ and $R_2 = 0.135$ and occupancies of 2.90(4), 7.4(3), and 2.2(2) at Cs, Na, and Xe(3), respectively. Inclusion of another peak opposite a four-ring in the large cavity as Xe(2) further reduced the error indices to 0.092 and 0.115 with resulting occupancies of 2.91(3), 8.1(2), 1.13(9), and 1.04(9) at Cs, Na, Xe(2), and Xe(3), respectively. When this model was refined with fixed occupancies of 3.0 and 8.0 (their maximum values by symmetry) at Cs and Na, and 1.0 each at Xe(2) and Xe(3), the error indices became $R_1 = 0.093$ and $R_2 = 0.116$. Similarly, from the subsequent difference Fourier function based on this model, a peak at (0.0,0.0,0.0) was introduced as Xe(1). This model converged to $R_1 = 0.082$ and $R_2 = 0.091$ with an occupancy of 0.51(4) at Xe(1). The final cycles of refinement with all occupancies fixed at 3.0, 8.0, 0.5, 1.0, and 1.0 for Cs, Na, and Xe(*i*), $i = 1-3$, respectively, and with anisotropic thermal parameters for all atoms converged to $R_1 = 0.056$ and $R_2 = 0.059$. The final structural parameters for this crystal, Cs_3-A(2.5Xe), are given in Table 1a. Selected interatomic distances and angles are given in Table 2.

Cs_3-A(4.5Xe) (Crystal 2). Full-matrix least-squares refinement began with the atomic parameters of the zeolite framework atoms and the cations in Cs_3-A(2.5Xe) (crystal 1). Anisotropic refinement converged to $R_1 = 0.19$ and $R_2 = 0.27$. A refinement with Xe(2) at a peak (0.320,0.320,0.5) in an ensuing difference Fourier function converged to $R_1 = 0.12$ and $R_2 = 0.17$ with resulting occupancies of 2.82(6), 8.7(4), and 3.1(1) at Cs, Na, and Xe(2), respectively. Another difference Fourier function based on this model revealed a peak deep in the large cavity at (0.361,0.361,0.361). The following refinement with this peak as Xe(3) converged with $R_1 = 0.100$ and $R_2 = 0.117$, resulting in occupancies of 3.11(4), 7.9(3), 2.1(1), and 3.9(1) at Cs, Na, Xe(2), and Xe(3), respectively. When this model was refined with fixed occupancies of 3.0 at Cs and 8.0 at Na (vide supra), the occupancies at Xe(2) and Xe(3) converged to 2.03(9) and 4.00(11) with $R_1 = 0.100$ and $R_2 = 0.118$. A subsequent refinement including a peak found at the center of the sodalite unit at (0.0,0.0,0.0) as Xe(1) further reduced the error indices to $R_1 = 0.087$ and $R_2 = 0.088$ with refined occupancies of 0.82(4), 2.29(7), and 1.64(7) at Xe(*i*), $i = 1-3$, respectively. Finally, a refinement with anisotropic thermal parameters for all atoms converged with $R_1 = 0.061$ and $R_2 = 0.058$ and occupancies of 0.77(3), 2.09(5), and 1.66(5) at Xe(*i*), $i = 1-3$, respectively. The final cycles of refinement with all occupancies fixed at 3.0, 8.0, 0.75, 2.0, and 1.75 for Cs, Na, and Xe(*i*), $i = 1-3$, respectively, converged with no further changes in the error indices. The final structural parameters for this crystal, Cs_3-A(4.5Xe), are given in Table 1b. Selected interatomic distances and angles are given in Table 2.

Cs_3-A(5.25Xe) (Crystal 3). Full-matrix least-squares refinement began with the atomic parameters of the zeolite framework atoms and of the cations in Cs_3-A(2.5Xe) (crystal 1), this model converged to $R_1 = 0.21$ and $R_2 = 0.31$ with resulting occupancies of 3.7(1) and 6.7(8) at Cs and Na, respectively. A refinement with Xe(2) at a Fourier peak (0.318,0.318,0.5)

TABLE 2: Selected Interatomic Distances (Å) and Angles (deg)[a]

	(a) Cs_3-A(2.5Xe) (crystal 1)	(b) Cs_3-A(4.5Xe) (crystal 2)	(c) Cs_3-A(5.25Xe) (crystal 3)
(Si,Al)−O(1)	1.651(5)	1.655(7)	1.654(6)
(Si,Al)−O(2)	1.648(8)	1.649(9)	1.647(8)
(Si,Al)−O(3)	1.674(5)	1.680(7)	1.672(6)
Na(1)−O(3)	2.286(8)	2.290(9)	2.271(9)
Na(1)−O(2)	2.935(7)	2.948(7)	2.939(7)
Na(2)−O(3)			2.636(56)
Na(2)−O(2)			3.166(83)
Cs−O(1)	3.399(12)	3.391(18)	3.420(15)
Cs−O(2)	3.581(6)	3.573(10)	3.567(9)
Xe(3)−Na(1)	3.18(2)	3.22(2)	3.38(2)
Xe(1)−Na(1)	4.297(4)	4.353(7)	4.277(7)
Xe(4)−Na(1)			4.04(3)
Xe(2)−Na(1)	4.08(1)	4.03(1)	4.08(1)
Xe(3)−Na(2)			5.10(8)
Xe(1)−Na(2)			5.34(5)
Xe(4)−Na(2)			3.61(5)
Xe(2)−Na(2)			3.18(8)
Xe(2)−Cs	4.45(2)	4.45(2)	4.44(2)
Xe(3)−Cs	5.02(2)	5.03(2)	5.03(2)
Xe(1)−O(3)	4.577(7)	4.57(1)	4.556(9)
Xe(4)−O(3)			3.94(3)
Xe(1)−O(2)	5.077(6)	5.09(1)	5.085(9)
Xe(4)−O(2)			3.81(2)
Xe(2)−O(1)	3.94(2)	3.91(3)	3.90(2)
Xe(2)−O(3)	3.95(1)	3.93(2)	3.92(1)
Xe(3)−O(3)	4.17(2)	4.24(2)	4.33(2)
Xe(3)−O(2)	4.44(3)	4.50(3)	4.58(2)
Xe(3)−Xe(2)	4.54(4)	4.51(3)	4.45(2)
Xe(2)−Xe(2)		5.77(3)	5.78(3)
O(1)−(Si,Al)−O(2)	108.4(5)	107.8(7)	108.4(6)
O(1)−(Si,Al)−O(3)	111.6(4)	111.9(6)	112.2(4)
O(2)−(Si,Al)−O(3)	106.8(2)	106.8(3)	106.9(3)
O(3)−(Si,Al)−O(3)	110.2(3)	109.9(5)	109.9(5)
(Si,Al)−O(1)−(Si,Al)	146.3(8)	145.8(12)	147.8(10)
(Si,Al)−O(2)−(Si,Al)	162.9(4)	163.3(6)	163.7(4)
(Si,Al)−O(3)−(Si,Al)	142.9(4)	142.8(3)	142.6(3)
O(3)−Na(1)−O(3)	118.1(2)	117.4(5)	118.1(5)
Xe(1)−Na(1)−O(3)	82.0(2)	80.6(3)	82.0(3)
Xe(4)−Na(1)−O(3)			82.0(3)
Xe(3)−Na(1)−O(3)	98.0(3)	99.5(4)	98.0(5)
Xe(1)−Na(1)−Xe(3)	180.0[b]	180.0[b]	180.0[b]
Xe(4)−Na(1)−Xe(3)			180.0[b]
O(3)−Na(2)−O(3)			95.3(6)
Xe(1)−Na(2)−O(3)			58.6(7)
Xe(4)−Na(2)−O(3)			58.6(7)
Xe(2)−Xe(3)−Xe(2)		95.1(5)[c], 79.4(4)[d]	97.3(4)[c], 81.1(4)[e]
Xe(3)−Xe(2)−Xe(3)		84.9(5)[f]	82.7(4)[f]

[a] The numbers in parentheses are the estimated standard deviations in the units of the least significant digit given for the corresponding parameter. [b] Exactly 180° by symmetry. [c] For the rhombus of four xenon atoms. [d] For the three-Xe arrangement. [e] For the trigonal-bipyramidal arrangement of five xenon atoms. [f] Required to be the supplement of the Xe(2)−Xe(3)−Xe(2) angle.

observed opposite a four-ring in the large cavity converged with $R_1 = 0.14$ and $R_2 = 0.22$, resulting in occupancies of 2.94(7), 8.7(5), and 3.5(2) at Cs, Na, and Xe(2), respectively. Another difference Fourier function based on a model with occupancy at Cs fixed at 3.0 revealed peaks at (0.233,0.233,0.233) and (0.351,0.351,0.351) on 3-fold axes in the large cavity. The following refinement including these peaks as Na(2) and Xe(3), respectively, converged with $R_1 = 0.11$ and $R_2 = 0.15$ and occupancies of 6.0(3), 1.5(2), 2.0(1), and 4.1(1) at Na(1), Na(2), Xe(2), and Xe(3), respectively. A subsequent difference Fourier function based on this model revealed two peaks in the sodalite unit: at (0.0,0.0,0.0) at the center and (0.039,0.039,0.039) on a 3-fold axis. Refinement including these peaks as Xe(1) and Xe(4), respectively, converged to $R_1 = 0.061$ and $R_2 = 0.056$, resulting in occupancies of 6.1(2), 1.7(1), 0.72(2), 2.26(6), 2.15(6), and 0.22(2) at Na(1), Na(2), and Xe(i), $i = 1-4$, respectively. The final cycles of refinement with all occupancies fixed at 3.0, 6.5, 1.5, 0.75, 2.25, 2, and 0.25, respectively, at Cs, Na(1), Na(2), and Xe(i), $i = 1-4$, and with anisotropic thermal parameters for all atoms, converged to the error indices $R_1 = 0.061$ and $R_2 = 0.057$. The final structural parameters for this crystal, Cs_3-A(5.25Xe), are given in Table 1c. Selected interatomic distances and angles are given in Table 2.

The values of the goodness-of-fit, $(\sum w(F_o - |F_c|)^2/(m - s))^{1/2}$, are 1.87, 1.95, and 2.21, respectively, for crystals 1, 2, and 3; similarly the number of observations, m, are 225, 191, and 216, and the number of parameters, s, are 34, 34, and 40. All shifts in the final cycles of refinement were less than 0.1% of their corresponding estimated standard deviations. The quantity minimized in least-squares is $\sum w(F_o - |F_c|)^2$, where the weights (w) are the reciprocal squares of $\sigma(F_o)$, the standard deviation of each observed structure factor. Atomic scattering factors for Cs^+, Xe, Na^+, O^-, and $(Si,Al)^{1.75+}$ were used.[42,43] The function describing $(Si,Al)^{1.75+}$ is the mean of the Si^{4+}, Si^0, Al^{3+}, and Al^0 functions. All scattering factors were modified to account for anomalous dispersion.[44,45]

Results and Discussion

Zeolite A Framework and Cations. The structural parameters of the framework atoms and cations are almost identical in all six of the following structures: empty Cs_3-A,[27] Cs_3-A(xXe), $x = 2.5$ and 4.5 (crystals 1 and 2), Cs_3-A(xAr), $x = 5$ and 6,[29] and Cs_3-A(5Kr).[28] The same is true for the framework atoms, Cs^+ ions, and most Na^+ ions in Cs_3-A(5.25Xe) (crystal 3); the positions of the remaining six-ring Na^+ ions are, however, quite different.

In the crystal structures of Cs_3-A(2.5Xe), Cs_3-A(4.5Xe), and 75% of the unit cells of Cs_3-A(5.25Xe), eight Na^+ ions per unit cell fully occupy the six-ring centers (see Tables 1 and 3). Each Na^+ ion is 2.286(8) Å from three O(3) oxygens in crystal 1, 2.290(9) Å in crystal 2, and 2.271(9) Å in most unit cells of crystal 3. These Na^+ ions extend 0.32, 0.38, and 0.32 Å into the large cavity from the (111) planes at O(3), respectively (see Table 4). The O(3)−Na−O(3) angles are close to 120° (118.1(2)°, 117.4(5)°, and 118.1(5)°, respectively, in the three crystals), so the Na^+ ions are nearly trigonal-planar. In the remaining 25% of the unit cells of Cs_3-A(5.25Xe), two of the eight Na^+ ions per unit cell are located at positions similar to those in crystals 1 and 2. The other six Na^+ ions, at Na(2), extend much more deeply, 1.38 Å, into the large cavity from the (111) planes at O(3) (see Table 4). Concomitantly, each of these six Na^+ ions is also much further, 2.64(6) Å, from its three O(3) oxygens. These Na^+ ions appear to be interacting strongly with the Xe(2) atoms, the equatorial Xe atoms of the trigonal-bipyramidal Xe_5 clusters in the large cavities (vide infra).

The occupancies of the Cs^+ ions in the eight-rings of the three Xe-encapsulate structures herein reported are slightly greater (closer to integral) than they were in Cs_3-A and Cs_3-A(5Kr),[27,28] due to the (purposefully) higher Cs^+/Na^+ ratio in the ion-exchange solution used for the preparation of Cs_3-A in this work and for Cs_3-A(xAr), $x = 5$ and 6.[29]

In these Xe-encapsulate structures, three Cs^+ ions per unit cell fully occupy the centers of the eight-rings at equipoints of local symmetry C_{4h} (D_{4h} in $Pm3m$), positions commonly found in partially or fully Cs^+-exchanged zeolite A.[27−29,46−49] Each Cs^+ ion is 3.399(12) Å from four O(1) oxygens and 3.581(6) Å from four O(2) oxygens in Cs_3-A(2.5Xe), 3.391(18) and

TABLE 3: Distribution of Cations and Xe Atoms in Cs_3-A(xXe)

crystals	Cs_3-A(2.5Xe), crystal 1			Cs_3-A(4.5Xe), crystal 2			Cs_3-A(5.25Xe), crystal 3		
unit cell	1	2	mean	1	2	mean	1	2	mean
population (%)	50	50		75	25		75	25	
Cs[a]	3	3	3	3	3	3	3	3	3
Na(1)[b]	8	8	8	8	8	8	8	2	6.5
Na(2)[c,d]								6	1.5
Xe(1)[e]	1	0	0.5	1	0	0.75	1		0.75
Xe(4)[c,f]								1	0.25
Xe(2)[d,g]	1	1	1	2	2	2	2	3	2.25
Xe(3)[c,d]	1	1	1	2	1	1.75	2	2	2

[a] At the center of an eight-ring. [b] Near the center of a six-ring. [c] Opposite a six-ring. [d] In the large cavity. [e] At the center of a sodalite unit. [f] In the sodalite unit. [g] Opposite a four-ring.

TABLE 4: Deviations of Atoms (Å) from the (111) Plane at O(3)[a]

	(a) Cs_3-A(2.5Xe) (crystal 1)	(b) Cs_3-A(4.5Xe) (crystal 2)	(c) Cs_3-A(5.25Xe) (crystal 3)
Na(1)	0.32	0.38	0.32
Na(2)			1.38
Xe(1)	−3.98	−3.98	−3.96
Xe(3)	3.50	3.60	3.70
Xe(4)	3.50	3.60	−2.23[b]

[a] A negative deviation indicates that the atom lies on the same side of the plane as the origin, i.e., inside the sodalite unit. [b] 1.73 Å from the origin (center of the sodalite unit).

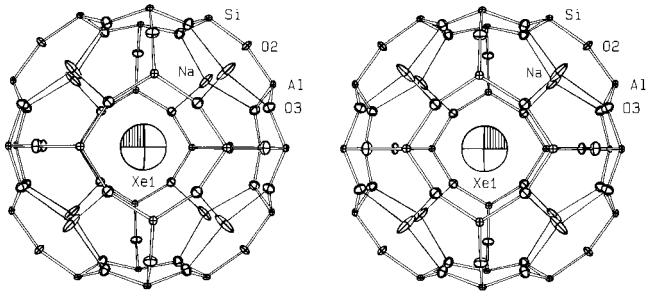

Figure 1. Stereoview of a sodalite unit in the unit cell 1 of Cs_3-A(5.25Xe), showing an encapsulated Xe atom located at the center. The zeolite A framework is drawn with open bonds between oxygens and tetrahedrally coordinated (Si,Al) atoms. Ellipsoids of 20% probability are shown.

3.573(10) Å in Cs_3-A(4.5Xe), and 3.420(15) and 3.567(9) Å, respectively, in Cs_3-A(5.25Xe) (see Table 2). Although these distances are substantially longer than the sum, 2.99 Å, of the conventional ionic radii of O^{2-} and Cs^+,[50,51] these positions are well established experimentally[27−29,46−49] and theoretically.[52,53]

As in the previously reported crystal structures of Cs_3-A(5Kr) and Cs_3-A(xAr), $x = 5$ and 6, the 12th cation per unit cell is assumed to be, at least predominantly, a H^+ ion, because it could not be located crystallographically.[27−29] Alternatively, it may have been lost as water.[27−29]

Xenon Atom in the Sodalite Unit. In Cs_3-A(2.5Xe), half of the sodalite units are empty. In the other half, a xenon atom is found at Xe(1), at the center of the sodalite unit (see Tables 3 and 4). Only 25% of the unit cells of Cs_3-A(4.5Xe) are empty; the remaining 75% contain a xenon atom at Xe(1). In Cs_3-A(5.25Xe), however, all sodalite units contain a xenon atom: 75% are at Xe(1) and each of the remainder is 1.73 Å away at Xe(4), on a 3-fold axis opposite a six-ring (see Figures 1 and 2).

A theoretical calculation indicated that a xenon atom in a sodalite unit containing Na^+ ions should find an energy minimum at its center,[14] at Xe(1), where most of the sodalite-unit xenon atoms are found in this work. Note, however, because

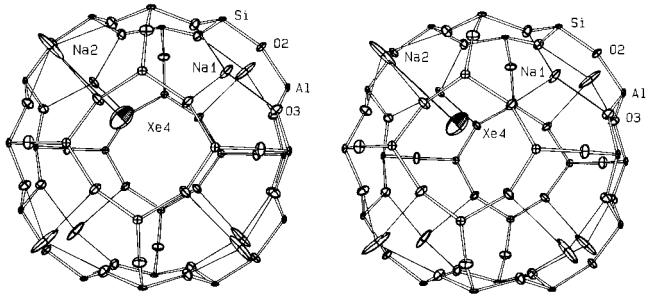

Figure 2. Stereoview of a sodalite unit in the unit cell 2 of Cs_3-A(5.25Xe), showing an encapsulated Xe atom near its center on a 3-fold axis. See the caption to Figure 1 for other details.

Xe(1) is at a crystallographic inversion center that the electrostatic field gradient must be zero and the xenon atom can be polarized only when it vibrates away from this position.

The xenon atom at Xe(1) is 4.277(7) and 4.556(9) Å, respectively, from the nearest Na^+ ions and six-ring oxygens in Cs_3-A(5.25Xe); similar distances are seen in crystals 1 and 2. These long distances indicate an absence of appreciate bonding character. Each xenon atom at Xe(4) (in Cs_3-A(5.25Xe)) is, however, 4.04(3) Å from a Na^+ ion at Na(1) and 3.94(3) Å from three O(3) oxygens. The occupancy at Xe(4) must be a result of the higher loading of xenon atoms in the large cavities: the Na^+ ions have become nonequivalent, so some sodalite units can have their eight Na^+ ions arranged asymmetrically, causing some sodalite-unit Xe atoms (Xe(4)) to be off center.

Xenon Atoms in the Large Cavity. The 2, 3.75, and 4.25 atoms of xenon in each large cavity of Cs_3-A(2.5Xe), Cs_3-A(4.5Xe), and Cs_3-A(5.25Xe), respectively, are found at two crystallographically distinct positions. That there are two kinds of positions indicates that the xenon atoms are not arranging themselves by simple packing within the highly symmetric zeolites, to form, for example, a tetrahedron. It is attributed to dipolar interactions among the sorbed atoms (vide infra). In Cs_3-A(2.5Xe), one Xe atom at Xe(2) lies opposite a four-ring, and another Xe atom at Xe(3) lies on a 3-fold axis opposite a six-ring (see Figure 3 and Table 3). Similarly, two xenon atoms at each position (Xe(2) and Xe(3)) are found in 75% of the unit cells of Cs_3-A(4.5Xe), with two at Xe(2) and only one at Xe(3) in the remainder (see Figures 4 and 5 and Table 4). In Cs_3-A(5.25), there are two atoms at Xe(3) and 2.25 at Xe(2), which means that 75% of the unit cells have two Xe atoms at Xe(2) and the remaining 25% have three (see Figure 6 and Table 3).

The closest approaches of these xenon atoms to nonframework cations are 3.18(2), 3.22(2), and 3.38(2) Å for Xe(3)−Na^+ and 4.45(2), 4.45(2), and 4.44(2) Å for Xe(2)−Cs^+ ions, while those to framework oxygens (Xe(2)−O(1)) are 3.94(2), 3.91(3), and 3.90(2) Å, respectively, for Cs_3-A(xXe), $x = 2.5$,

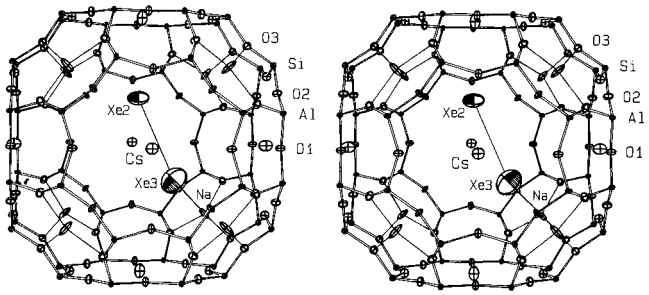

Figure 3. Stereoview of the large cavity of Cs_3-A(2.5Xe) with two Xe atoms at Xe(2) and Xe(3). The most significant interactions among Xe atoms, and those between Xe and Na^+ ions and framework oxygens, are indicated by fine solid lines.

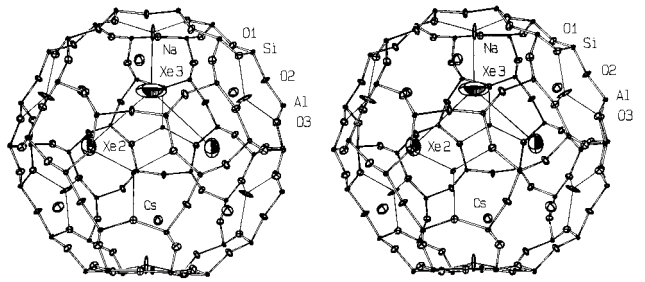

Figure 4. Stereoview of the large cavity of Cs_3-A(4.5Xe) with three Xe atoms at Xe(2) and Xe(3). See the captions to Figures 1 and 3 for other details.

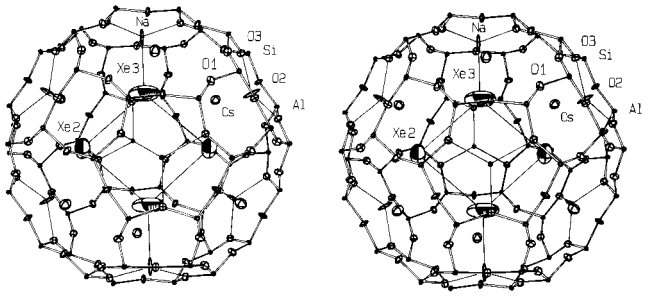

Figure 5. Stereoview of the large cavity of Cs_3-A(4.5Xe) with the only reasonable (except for orientation) arrangement of four Xe atoms at Xe(2) and Xe(3). The four-xenon rhombus (nearly a square) is planar. See the captions to Figures 1 and 3 for other details.

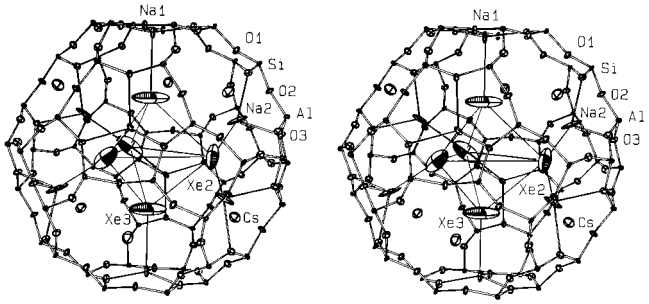

Figure 6. Stereoview of the large cavity of Cs_3-A(5.25Xe) with the only reasonable (except for orientation) arrangement of three Xe atoms at Xe(2) and two at Xe(3). The five xenon atoms have a trigonal-bipyramid arrangement. See the captions to Figures 1 and 3 for other details.

4.5, and 5.25 (see Table 2). Considering the radii of the cations (r_{Na^+} = 0.97 Å and r_{Cs^+} = 1.67 Å),[50,51] framework oxygens (1.32 Å),[50,51] and xenon atoms (2.18 Å as $r_{min}/2$[30] and as found in the solid[54]), some of the xenon atoms are sufficiently close to their neighbors to be considered as having relatively strong interactions. In particular, when the distances are compared to the sum of the above radii for Na^+ and Xe, 0.97 + 2.18 = 3.15 Å, the approach distances of the 3-fold-axis xenon atoms, Xe(3), to the six-ring Na^+ ions (3.18(2), 3.22(2), and 3.38(2) Å in Cs_3-A(*x*Xe), *x* = 2.5, 4.5, and 5.25, respectively) indicate relatively strong Na^+−Xe interactions. In contrast, inter-xenon distances of 4.54(4), 4.51(3), and 4.45(2) Å between Xe(2) and Xe(3) in the corresponding large cavities (vide infra) are nearly an ångstrom larger than those in solid Xe.[54]

Cs^+−Xe interactions are much less important than Na^+−Xe interactions in these structures, as would be expected because Cs^+ is much larger than Na^+, so the electric field gradient at its "surface" is much less. The shortest Cs^+−Xe distances in the three structures, ca. 4.45 Å (see Table 2), are ca. 0.60 Å longer than the sum of the Cs^+ and Xe radii.[50,51,54] In contrast, the shortest Na^+−Xe distances, ca. 3.20 Å, are near to (only 0.05 Å longer than) the corresponding sum.

The xenon atoms at Xe(3) in the large cavities of both Cs_3-A(*x*Xe), *x* = 2.5 and 4.5, and in 75% of the large cavities of Cs_3-A(5.25Xe), appear to interact much more strongly with six-ring Na^+ ions than do those at Xe(1). These Xe(3)−Na^+ interactions (3.18(2), 3.22(2), and 3.38(2) Å, respectively) are all shorter than the corresponding Xe(1)−Na^+ distances (4.297(4), 4.353(7), and 4.277(7) Å). Similarly, the large-cavity Ar and Kr atoms in Cs_3-A(5Kr)[28] and Cs_3-A(*x*Ar),[29] *x* = 5 and 6, respectively, interact more strongly with Na^+ ions than do the small-cavity Ar or Kr's. The Xe(3)−O(3) distances (4.17(2), 4.24(2), and 4.33(2) Å, respectively) are also generally shorter than the Xe(1)−O(3) distances (4.577(7), 4.57(1), and 4.556(9) Å, respectively) in Cs_3-A(*x*Xe), *x* = 2.5, 4.5, and 5.25, respectively.

Xenon Clusters. The two xenon atoms at Xe(2) and Xe(3) on the inner surface of the large cavity in Cs_3-A(2.5Xe) may be placed within their partially occupied equipoints in various ways. The shortest possible inter-xenon distance, Xe(2)−Xe(3) = 1.95(2) Å, is impossibly short and is dismissed. Another inter-xenon distance, 4.54(4) Å, suggests the possibility of an Xe(2)−Xe(3) interaction with favorably oriented induced dipoles (see Figure 3). A longer distance, 6.12(3) Å, is also possible.

Such dipoles induced on Xe atoms by the electric fields present within zeolites are the physical basis of one of the chemical-shift terms used to interpret the NMR spectra of intrazeolitic Xe.[1−3,5,55−59] The δ_E term "expresses the effect of electrical charges (electric fields created by the cations and by the negative charges of the lattice, polarizability and van der Waals interactions)".[58] These induced dipoles are consistent with the arrangements of the less polarizeable Kr and Ar atoms seen in their high-pressure encapsulates in Cs-A.[28,29] NMR work is planned on the Xe encapsulates reported here.

The four xenon atoms at Xe(2) and Xe(3) on the inner surface of the large cavity of unit cell 1 (75% occupancy, see Table 3) of Cs_3-A(4.5Xe) may be placed similarly. The shortest possible inter-xenon distances, Xe(2)−Xe(3) = 1.95(1) Å, Xe(2)−Xe(2) = 3.33(2) Å, and Xe(3)−Xe(3) = 3.52(5) Å, are impossibly short and are dismissed. A distance found among the equipoints of Xe(3), 4.97(4) Å, suggests the possibility of an Xe(3)−Xe(3) interaction, but this is dismissed because the dipoles induced on this pair of Xe(3) atoms are oriented unfavorably. The next set of distances Xe(2)−Xe(2) = 4.71(6) and Xe(2)−Xe(3) = 4.51(2) Å offer two solutions. (Longer distances, corresponding to atoms on near opposite sides of the large cavity, require impossibly short distances to complete a model and are dismissed.) Of the two possible solutions, a planar four-Xe ring arrangement, [−Xe(2)−Xe(3)−Xe(2)−Xe(3)−], with Xe(2)−Xe(3) = 4.51(3) Å and Xe(2)−Xe(3)−Xe(2) = 95.1(5)°, is selected as the most plausible due to its higher

symmetry and favorably oriented induced dipoles (see Figure 5), as discussed previously.[28,29] In this rhombus, Xe atoms alternately approach Na^+ ions and four-oxygen rings and are polarized oppositely, allowing their inter-xenon approaches to be attractive. These interactions are actually shorter and therefore stronger than the corresponding interactions in Cs_3-A(xAr), x = 5 and 6,[29] and Cs_3-A(5Kr).[28]

The two xenon atoms at Xe(2) and one at Xe(3) in the large cavity of unit cell 2 (25% occupancy) of Cs_3-A(4.5Xe) may also be placed at various positions. The shortest distance, Xe(2)−Xe(3) = 1.95(1) Å, is again impossibly short. Of the two longer Xe(2)−Xe(3) distances, 4.51(3) and 6.07(2) Å, the first indicates a reasonable interaction. Possible Xe(2)−Xe(2) interactions are 4.71(6), 5.77(3), and 6.66(4) Å. Among these, a planar three-Xe arrangement, [Xe(2)−Xe(3)−Xe(2)], with Xe(2)−Xe(3) = 4.51(3) Å, Xe(2)−Xe(2) = 5.77(3) Å, and Xe(2)−Xe(3)−Xe(2) = 79.4(4)° is selected as the most plausible due to its higher symmetry and favorably oriented induced dipoles (see Figure 4). In this three-Xe arrangement, xenon atoms alternately approach Na^+ ions and four-oxygen rings; they are therefore polarized oppositely, allowing their inter-xenon approaches to be attractive.

The most favorable arrangement of four xenon atoms in 75% of the large cavities of Cs_3-A(5.25Xe) is a rhombus as seen in unit cell 1 of Cs_3-A(4.5Xe) and as discussed previously.[28,29] In this rhombus, the most plausible arrangement is a planar four-Xe ring arrangement, [−Xe(2)−Xe(3)−Xe(2)−Xe(3)−], Xe(2)−Xe(3) = 4.45 Å and Xe(2)−Xe(3)−Xe(2) = 97.3(4)° (see Figure 5).

The five xenon atoms in the large cavity of unit cell 2 (25% occupancy, see Table 3) of Cs_3-A(5.25Xe), three at Xe(2) and two at Xe(3), may also be placed within their partially occupied equipoints in various ways. The shortest inter-xenon distance, 1.94(1) Å for Xe(2)−Xe(3), is dismissed as above. The closest interactions between equivalent xenon atoms, 3.39(5) Å for Xe(3)−Xe(3) and 3.34(2) Å for Xe(2)−Xe(2), are dismissed because their induced dipoles are oriented unfavorably, also as above. The next longest inter-xenon distance, 4.45(2) Å for Xe(2)−Xe(3), is plausible. However, various arrangements remain possible. A trigonal-bipyramidal arrangement is selected as most plausible because of its higher symmetry and by considerations regarding alternating polarizations of xenon atoms as before with Cs_3-A(4.5Xe) (see Figures 6). Two Xe(3) atoms on a single 3-fold axis on opposite sides of the large cavity occupy axial positions and three Xe(2) atoms are at equatorial positions with inter-xenon distances of 4.45(2) Å for Xe(2)−Xe(3) and 5.78(3) Å for Xe(2)−Xe(2). In this arrangement, ϵ^- polarizations from all three Xe(2) atoms point toward the center of the large cavity where each can interact with each of the two δ^+ polarizations from the 3-fold-axis Xe(3) atoms. The six Na^+ ions in unit cell 2 do not interact with the axial Xe(3) atoms; instead, they extend deeply into the large cavity to interact very strongly with the three ϵ^- polarized Xe(2) atoms of the Xe_5 cluster; the Xe(2)−Na(2) distance is only 3.18(8) Å (see Figure 7). Such an extension of six-ring cations into the large cavity due to interactions with adsorbate was previously observed in Zn^{2+}-exchanged zeolite Y.[60] In this trigonal-bipyramidal arrangement of five xenon atoms, the favorable Xe(2)−Xe(3) interactions, 4.45(2) Å, are nicely much shorter than the unfavorable equatorial Xe(2)−Xe(2) interactions, 5.78(4) Å.

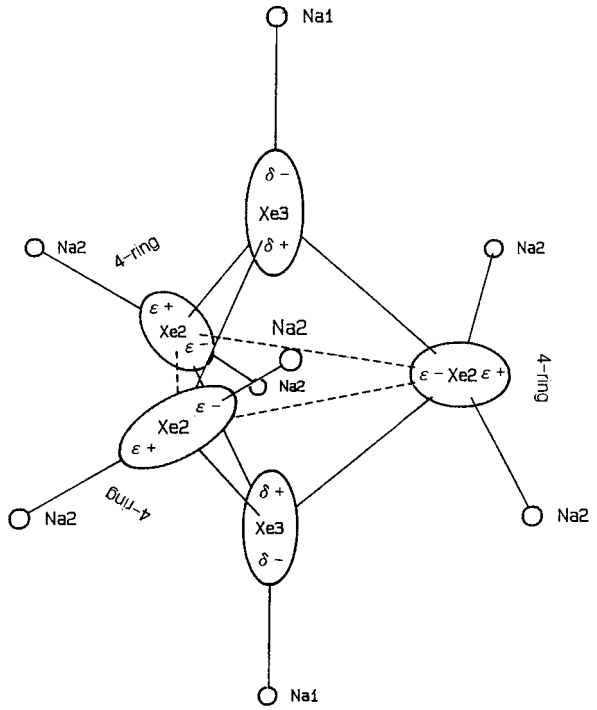

Figure 7. Schematic diagram of the trigonal bipyramid of five xenon atoms and six Na^+ ions at Na(2) in the large cavities of Cs_3-A(5.25Xe). The immediate environment of each Xe atom and the dipole moment it induces on each Xe are shown. The favorable interactions between the polarized Xe atoms are indicated by fine lines and the unfavorable ones by dashed.

General Discussion

To date, the following rare-gas encapsulates in Cs_3-A have been studied by single-crystal X-ray diffraction methods: Cs_3-A(xAr), x = 5 and 6,[29] Cs_3-A(5Kr),[28] and Cs_3-A(xXe), x = 2.5, 4.5, and 5.25 (this work). The framework and the cation positions are very much the same in all of these structures except for Cs_3-A(5.25Xe) whose six-ring Na^+ ions are no longer equivalent, probably a consequence of the high polarizability of Xe as compared to Ar and Kr.

In all cases, although the gas atoms are somewhat to substantially larger than the nominal size of the six-ring window (ca. 2.2 Å in diameter), rare-gas atoms were always found in sodalite units. However, these sodalite-unit rare-gas atoms appear to interact less strongly with the six-ring Na^+ ions than do those found in the large cavities of all crystals. In the large cavity, a single Na^+ ion can induce a strong dipole on a rare-gas atom; in the sodalite unit, a rare-gas atom can interact with three or more Na^+ ions which are, of course, not arranged to induce a simple dipole, so the interaction is weaker and the distances longer.

The number of rare-gas atoms encapsulated in the large cavity are four in Cs_3-A(5Ar),[29] five in Cs_3-A(6Ar),[29] four in Cs_3-A(5Kr),[28] two in Cs_3-A(2.5Xe), three or four in Cs_3-A(4.5Xe), and four or five in Cs_3-A(5.25Xe). These encapsulated atoms are all near the inner surface of the cavity. When there are four such atoms they form a rhombus stabilized by alternating dipoles induced by four-ring oxygens and six-ring Na^+ ions. Similarly, when there are five, they form a trigonal bipyramid: two X(3) atoms, X = Ar or Xe, on a single 3-fold axis on opposite sides of the large cavity occupy axial positions and three X(2) atoms, X = Ar or Xe, are at equatorial positions. In this arrangement, ϵ^- polarizations from all three X(2) atoms point toward the center of the large cavity where each can interact with both δ^+ polarizations from the 3-fold-axis X(3) atoms.

In all structures, the approach distances of these rare-gas atoms to six-ring Na^+ ions and four-ring oxygens are substantially longer than the sum of the corresponding ionic radii and

the rare-gas atomic radii. However, considering for the moment only those large cavities that have encapsulated rhombuses, when the 2.91(5), 3.23(2), and 3.22(2) Å distances for Ar(3)−Na^+, Kr(3)−Na^+, and Xe(3)−Na^+ in Cs_3-A(5Ar),[29] Cs_3-A(5Kr),[28] and Cs_3-A(4.5Xe), respectively, are compared to the corresponding sums of atomic and ionic radii, 2.89, 2.95, and 3.195 Å for Ar−Na^+, Kr−Na^+, and Xe−Na^+, respectively, it is seen that the Xe(3) atoms in the large cavity of Cs_3-A(4.5Xe) interact more strongly with the six-ring Na^+ ions than do the Kr(3) atoms in Cs_3-A(5Kr).[28] Similarly, in the large cavities with encapsulated trigonal bipyramids, when the 3.09(6) Å Ar(3)−Na^+ distance in Cs_3-A(6Ar)[29] and the 3.38(2) Å Xe(3)−Na^+ distance in Cs_3-A(5.25Xe) are compared to the corresponding sums, it is seen that the Xe(3) atoms in the large cavity of Cs_3-A(5.25Xe) interact more strongly with the six-ring Na^+ ions than do the Ar(3) atoms in Cs_3-A(5Ar). When the 2.91(5) and 3.09(6) Å Ar(3)−Na^+ distances in Cs_3-A(xAr), $x = 5$ and 6,[29] and the 3.18(2), 3.22(2), and 3.38(2) Å Xe(3)−Na^+ distances in Cs_3-A(xXe), $x = 2.5$, 4.5, and 5.25, are compared to the corresponding sums, it is seen that the more rare-gas atoms in the large cavity, the weaker the interactions of each with Na^+ become.

Similar comparisons of approach distances to four-ring oxygens, 3.93(4) vs 3.24 Å, 3.81(2) vs 3.30 Å, and 3.95(1), 3.93(2), 3.92(1) vs 3.545 Å for Ar(2)−O(3), Kr(2)−O(3) and Xe(2)−O(3), respectively, reveal that Xe(2) atoms in Cs_3-A(xXe), $x = 2.5$, 4.5, and 5.25, interact more strongly with the four-ring oxygens than do the Kr(2) atoms in Cs_3-A(5Kr);[28] the Ar(2) atoms in Cs_3-A(xAr), $x = 5$ and 6,[29] interact the least strongly with the four-ring oxygens.

These relative approach distances of rare-gas atoms to Na^+ ions and to framework oxygens are a consequence of two competing factors: atom size and atomic polarizability in the electrostatic fields within the zeolite cavity. Because argon is the smallest of the rare gases studied, and therefore the least polarizable, inter-argon interactions in the large cavity should be weaker than the corresponding inter-krypton or inter-xenon interactions. It follows from the above considerations that the argon atoms at Ar(3) should be able to approach Na^+ ions more closely than Kr or Xe. Those at Ar(2) are furthest (relatively) from the negative framework oxygens, perhaps because they cannot be simply polarized by the large four-rings. Similarly, the result that Xe atoms (which are the largest) approach six-ring Na^+ ions relatively more closely than Ar and Kr atoms, must be attributed to their much greater polarizability.

Acknowledgment. N.H.H. gratefully acknowledges the support of the Korean Science and Engineering Foundation for research funds (KOSEF 941-0300-027-2) and the Central Laboratory of Kyungpook National University for the diffractometer and computing facilities.

Supporting Information Available: Observed and calculated structure factors for Cs_3-A(2.5Xe), Cs_3-A(4.5Xe), and Cs_3-A(5.25Xe). This material is available free of charge via the Internet at http://pubs.acs.org.

References and Notes

(1) Ito, T.; Fraissard, J. *J. Chem. Phys.* **1982**, *76*, 5225−5229.
(2) Chen, Q. J.; Fraissard, J. *J. Phys. Chem.* **1992**, *96*, 1809−1814 and references therein.
(3) Gedeon, A.; Bonardet, J. L.; Ito, T.; Fraissard, J. *J. Phys. Chem.* **1989**, *93*, 2563−2569.
(4) Bansal, N.; Dybowski, C. *J. Phys. Chem.* **1988**, *92*, 2333−2337.
(5) Chen, Q. J.; Ito, T.; Fraissard, J. *Zeolites* **1991**, *11*, 239−243.
(6) Fraissard, J.; Ito, T.; de Menorval, L. C. *Proceedings of the 8th International Conference on Catalysis, Berlin*; Verlag Chemie: Dechema, Germany 1984.
(7) Gedeon, A.; Ito, T.; Fraissard, J. *Zeolites* **1988**, *8*, 376−380.
(8) de Menorval, L. C.; Raftery, D.; Liu, S. B.; Takegoshi, K.; Ryoo, R.; Pines, A. *J. Phys. Chem.* **1990**, *94*, 27−31.
(9) Ito, T.; Bonardet, J. L.; Fraissard, J.; Nagy, J. B.; Andre, C.; Gabelica, Z.; Derouane, E. G. *Appl. Catal.* **1988**, *43*(1), L1-L5.
(10) Li, Feng Yin; Berry, R. S. *J. Phys. Chem.* **1995**, *99*, 2459−2468.
(11) Jameson, C. J.; Jameson, A. K.; Gerald II, R.; de Dios, A. C. *J. Chem. Phys.* **1992**, *96*, 1676−1689.
(12) Jameson, C. J.; Jameson, A. K.; Baello, B. I.; Lim, H. M. *J. Chem. Phys.* **1994**, *100*(8), 5965−5976.
(13) Jameson, C. J.; Jameson, A. K.; Lim, H. M.; Baello, B. I. *J. Chem. Phys.* **1994**, *100*(8), 5977−5987.
(14) Barrer, R. M.; Vaughan, D. E. W. *J. Phys. Chem. Solids* **1971**, *32*, 731−743.
(15) Chan, Y.-C.; Anderson, R. B. *J. Catal.* **1977**, *50*, 319−329.
(16) Sesney, W. J.; Shaffer, L. H. U.S. Patent 3316691, 1967.
(17) Gesser, H. D.; Rochon, A.; Lemire, A. E.; Masters, K. J.; Raudsepp, M. *Zeolites* **1984**, *4*, 22−24.
(18) Fraenkel, D.; Lazar, R.; Shabtai, J. *Alternative Energy Sources*; Hemisphere: Washington, DC, 1979; Vol. 8, pp 3771−3802.
(19) Yoon, J. H.; Heo, N. H., *J. Phys. Chem.* **1992**, *96*, 4997−5000.
(20) Rho, B. R.; Kim, D. H.; Kim, J. T.; Heo, N. H. *Hwahak Konghak* **1991**, *29*, 407−416.
(21) Samant, M. G.; de Menorval, L. C.; Dalla Betta, R. A.; Boudart, M. *J. Phys. Chem.* **1988**, *92*, 3937−3938.
(22) Dooryhee, E.; Greaves, G. N.; Steel, A. T.; Townsend, R. P.; Carr. S. W.; Thomas, J. M.; Catlow, C. R. A. *Faraday Discuss. Chem. Soc.* **1990**, *89*, 119−136.
(23) Santikary, P.; Yashonath, S.; Ananthakrishna, G. *J. Phys. Chem.* **1992**, *96*, 10469−10477.
(24) Derouane, E. G.; Andre, J. M.; Lucas, A. A. *Chem. Phys. Lett.* **1987**, *137*, 336−340 and references therein.
(25) Derouane, E. G.; Nagy, J. B. *Chem. Phys. Lett.* **1987**, *137*, 341−344.
(26) The nomenclature refers to the contents of the *Pm*3*m* unit cell: e.g., Na_{12}-A represents $Na_{12}Si_{12}Al_{12}O_{48}$, and Cs_3Na_8H-A and Cs_3-A represent $Cs_3Na_8HSi_{12}Al_{12}O_{48}$.
(27) Cho, K. H.; Kwon, J. H.; Kim, H. W.; Park, C. S.; Heo, N. H. *Bull. Korean Chem. Soc.* **1994**, *15*, 297−304.
(28) Heo, N. H.; Cho, K. H.; Kim, J. T.; Seff, K. *J. Phys. Chem.* **1994**, *98*, 13328−13333.
(29) Heo, N. H.; Lim, W. T.; Seff, K. *J. Phys. Chem.* **1996**, *100*, 13725−13731.
(30) Breck, D. W. *Zeolite Molecular Sieves: Structure, Chemistry, and Uses*; John Wiley & Sons: New York, 1974; pp 634−641.
(31) Ratcliffe, C. I.; Ripmeester, J. A. *J. Am. Chem. Soc.* **1995**, *117*, 1445−1446.
(32) Fraenkel, D. *CHEMTECH* **1981**, *1*, 60−65.
(33) Fraenkel, D.; Shabtai, J. *J. Am. Chem. Soc.* **1977**, *99*, 7074−7076.
(34) Kwon, J. H.; Cho, K. H.; Kim, H. W.; Suh, S. H.; Heo, N. H. *Bull. Korean Chem. Soc.* **1993**, *14*, 583−588.
(35) Fraenkel, D. *J. Chem. Soc., Faraday Trans. 1* **1981**, *77*, 2029−2039.
(36) Fraenkel, D.; Ittah, B.; M. Levy, M. *J. Chem. Soc., Chem. Commun.* **1984**, 1391−1392.
(37) Charnell, J. F. *J. Crystal Growth* **1971**, *8*, 291−294.
(38) Cruz, W. V.; Leung, P. C. W.; Seff, K. *J. Am. Chem. Soc.* **1978**, *100*, 6997−7003.
(39) Mellum, M. D.; Seff, K. *J. Phys. Chem.* **1984**, *88*, 3560−3563.
(40) *International Tables for X-ray Crystallography*; Kynoch Press: Birmingham, England, 1974; Vol. IV, pp 61−66.
(41) Calculations were performed with Structure Determination System, *Molen*; Enraf-Nonius: The Netherlands, 1990.
(42) Doyle, P. A.; Turner, P. S. *Acta Crystallogr., Sect. A* **1968**, *24*, 390−397.
(43) *International Tables for X-ray Crystallography*; Kynoch Press: Birmingham, England, 1974; Vol. IV, pp 71−98.
(44) Cromer, D. T. *Acta Crystallogr.* **1965**, *18*, 17−23.
(45) *International Tables for X-ray Crystallography*; Kynoch Press: Birmingham, England, 1974; Vol. IV, pp 148−150.
(46) Heo, N. H.; Seff, K. *J. Am. Chem. Soc.* **1987**, *109*, 7986−7992.
(47) Vance, T. B., Jr.; Seff, K. *J. Phys. Chem.* **1975**, *79*, 2163-2167.
(48) Firor, R. L.; Seff, K. *J. Am. Chem. Soc.* **1977**, *99*, 6249−6253.
(49) Subramanian, V.; Seff, K. *J. Phys. Chem.* **1979**, *83*, 2166−2169.
(50) *Handbook of Chemistry and Physics*, 64th ed.; Chemical Rubber Co.: Cleveland, OH, 1983; p F-187.
(51) Shannon, R. D.; Prewitt, C. T., *Acta Crystallogr., Sect. B* **1969**, *25*, 925−946.
(52) Ogawa, K.; Nitta, M.; Aomura, K. *J. Phys. Chem.* **1978**, *82*, 1655−1660.

(53) Takaishi, T.; Hosoi, H. *J. Phys. Chem.* **1982**, *86*, 2089−2094.
(54) Emsley, J. *The Elements*, 2nd ed.; Clarendon Press: Oxford, UK, 1991; pp 212−213.
(55) Liu, S. B.; Fung, B. M.; Yang, T. C.; Hong, E. C.; Chang, C. T.; Shih, P. C.; Tong, F. H.; Chen, T. L. *J. Phys. Chem.* **1994**, *98*, 4393−4401.
(56) Ripmeester, J. A.; Ratcliffe, C. I. *J. Phys. Chem.* **1990**, *94*, 7652−7656.
(57) de Menorval, L. C.; Fraissard, J. P.; Ito, T. *J. Chem. Soc., Faraday Trans. 1* **1982**, *78*, 403−410.
(58) Ito, T.; Fraissard, J. *J. Chem. Soc., Faraday Trans. 1* **1987**, *83*, 451−462.
(59) Demarquay, J.; Fraissard, J. *Chemical Physics Lett.* **1987**, *136*, 314−318.
(60) Seidel, A.; Boddenberg, B. *Chem. Phys. Lett.* **1996**, *249*, 117−122.